A Record Nine Different Phases (Four Cubic, Two Hexagonal, and One Lamellar Lyotropic Liquid Crystalline and Two Micellar Solutions) in a Ternary Isothermal System of an Amphiphilic Block Copolymer and Selective Solvents (Water and Oil)

Paschalis Alexandridis,*,†,‡ Ulf Olsson,† and Björn Lindman†

Physical Chemistry 1, Center for Chemistry and Chemical Engineering, Lund University, S-221 00 Lund, Sweden, and Department of Chemical Engineering, State University of New York at Buffalo, Buffalo, New York 14260-4200

We report on a ternary isothermal system consisting of a poly(ethylene oxide)/poly(propylene oxide) (PEO/PPO) amphiphilic block copolymer, "water", and "oil" (where "water" and "oil" are selective solvents for the different blocks), which exhibits the richest structural polymorphism ever observed (in equilibrium) in mixtures containing amphiphiles (such as block copolymers, surfactants, or lipids). The microstructure resulting from the self-assembly of the PEO/PPO block copolymer can vary from normal (oil-in-water) micelles in solution, through all types of normal and reverse (water-in-oil) lyotropic liquid crystals (normal micellar cubic, normal hexagonal, normal bicontinuous cubic, lamellar, reverse bicontinuous cubic, reverse hexagonal, reverse micellar cubic), to reverse micelles, as the relative volume fraction of the apolar ("oil"-like) components increases over that of the polar ("water"-like) components. The structure in the liquid crystalline phases has been established with small-angle X-ray scattering; both the normal and the reverse bicontinuous cubic structures are consistent with the *Ia*3*d* crystallographic space group (and the Gyroid minimal surface), while the normal and reverse micellar cubic structures are consistent with the *Im*3*m* and *Fd*3*m* space groups, respectively. The self-assembly of amphiphilic block copolymer in selective solvents described here provides a link between the self-assembly of surfactants in water (and oil/cosurfactant) and the self-assembly of block copolymers in the absence of any solvent. Furthermore, the ability of the PEO/PPO amphiphilic block copolymers to attain diverse microstructures is of great importance to numerous practical applications, especially since such copolymers are commercially available (as poloxamers, Pluronics, or Synperonics).

Introduction

Amphiphilic (αμφιφιλος) molecules such as surfactants and lipids, having an affinity (φιλος) for both (αμφι) "water" and "oil", play a fundamental role in biology and find widespread technological applications because of their unique ability to self-organize at interfaces and in solution and thus modify interfacial properties and enhance compatibility or partition.[1] Surfactants and lipids in solution can form thermodynamically stable (spontaneous self-assembly) supramolecular assemblies such as micelles[2] (in aqueous solutions), microemulsions[3] (in multicomponent systems with water, oil, and, often, cosurfactant), and lyotropic liquid crystals (lamellar, hexagonal and cubic),[4] as well as kinetically stabilized vesicles.[5] Block copolymers can also express amphiphilic character: they are known to associate into micelles when dissolved in a selective solvent[6,7] and to attain a number of microstruc-

tures, such as lamellae, cylinders, and spheres[8,9] in the absence of any solvent ("dry") or in mixtures with homopolymers.

Block copolymers consisting of poly(ethylene oxide) (PEO) and poly(propylene oxide) (PPO) are an interesting class of amphiphiles, developed originally for use as surface active agents in aqueous solutions,[10] but shown to also form structures in the absence of any solvent.[11,12] Despite their commercial availability (under the generic name poloxamers and the trade names Pluronics and Synperonics) and many practical applications,[13,14] the aqueous solution properties (even basic ones, such as the critical micellization concentration, the micelle size, etc.) of these amphiphiles remained elusive for a long time and were resolved only during the last 5 years.[15–18] From the recent

* To whom correspondence should be addressed at the State University of New York. E-mail: palexand@eng.buffalo.edu.
† Lund University.
‡ State University of New York at Buffalo.
(1) Evans, D. F.; Wennerström, H. *The Colloidal Domain: Where Physics, Chemistry, Biology, and Technology Meet*; VCH Publishers: New York, 1994.
(2) Lindman, B.; Wennerström, H. *Top. Curr. Chem.* **1980**, *87*, 1.
(3) Sjöblom, J.; Lindberg, R.; Friberg, S. E. *Adv. Colloid Interface Sci.* **1996**, *95*, 125.
(4) Laughlin, R. G. *The Aqueous Phase Behavior of Surfactants*; Academic Press: London, 1994.
(5) Lacic, D. D. *Liposomes: from Physics to Applications*; Elsevier: Amsterdam 1993.

(6) Tuzar, Z.; Kratochvil, P. In *Surface and Colloid Science*; Matjevic, E., Ed.; Plenum Press: New York, 1993; Vol. 15.
(7) Alexandridis, P.; Hatton, T. A. In *The Polymeric Materials Encyclopedia*; Salamone, J. C., Ed.; CRC Press: Boca Raton, FL, 1996; p 743.
(8) Bates, F. S.; Schulz, M. F.; Khandpur, A. K.; Förster, S.; Rosedale, J. H.; Almdal, K.; Mortensen, K. *Faraday Discuss.* **1994**, *98*, 7.
(9) Lohse, D. J.; Hadjichristidis, N. *Curr. Opin. Colloid Interface Sci.* **1997**, *2*, 171.
(10) Schmolka, I. R. *Surf. Sci. Ser.* **1967**, *1*, 300.
(11) Ashman, P. C.; Booth, C. *Polymer* **1975**, *16*, 889.
(12) Mortensen, K.; Brown, W.; Jorgensen, E. *Macromolecules* **1995**, *28*, 1458.
(13) Edens, M. W. *Surf. Sci. Ser* **1996**, *60*, 185.
(14) Alexandridis, P. *Curr. Opin. Colloid Interface Sci.* **1996**, *1*, 490.
(15) Alexandridis, P.; Hatton, T. A. *Colloids Surf., A* **1995**, *96*, 1.
(16) Almgren, M.; Brown, W.; Hvidt, S. *Colloid Polym. Sci.* **1995**, *273*, 2.

spur of activity in this field came the realization that PEO/PPO block copolymers can self-assemble in water into lyotropic liquid crystals (having lamellar, hexagonal, or cubic structure, with one-, two-, or three-dimensional order, respectively),[18-22] similarly to common surfactants.[4]

An novel development in the field of amphiphilic block copolymers is the discovery that ternary isothermal systems consisting of a PEO/PPO block copolymer, "water", and "oil" (where "water" and "oil" are selective solvents for the PEO and PPO blocks, respectively) can exhibit a very rich structural polymorphism.[22-28] A number of PEO–PPO–PEO triblock copolymers have been identified which self-assemble under equilibrium conditions into a variety of lyotropic liquid crystalline microstructures consisting of spherical, cylindrical, or planar microdomains, of normal ("oil"-in-"water") or reverse ("water"-in-"oil") morphology and discrete or interconnected (bicontinuous) topology.[22-26] Such an ability to form many normal and reverse structures at the same temperature has never before been observed in ternary systems of common surfactants with water and oil. Furthermore, the variety of structures formed by a PEO/PPO block copolymer in the presence of solvents is much greater than that of a block copolymer of a given block composition in the absence of solvents or even in the presence of homopolymers.

For a PEO/PPO block copolymer of a given block composition and molecular weight, the types of structures obtained in the presence of selective solvents appear to be a function of the volume fraction of the polar ("water"-like)/apolar ("oil"-like) components; this we have attributed to the ability of the macromolecular blocks to swell to a different extent (based on the amount of solvents available) with the respective solvents and to thus modulate the interfacial "curvature" and resulting structure.[25] The quality of the solvent and its ability to swell the different blocks will of course affect the phase behavior and structure, as a recent study of ours suggests.[26,27] In block copolymer melts, an increase in the copolymer molecular weight for a given A/B block composition increases the block segregation and the tendency for organization. To examine the effects of copolymer molecular weight on the self-assembly of amphiphilic block copolymers in the presence of selective solvents, we undertook a study of a group of PEO/PPO block copolymers having the same, roughly symmetric (40% PEO), block composition and varying molecular weight, under the same solvent conditions. We report here our results on the phase behavior and structure of the $(EO)_{19}(PO)_{43}(EO)_{19}-{}^2H_2O-p$-xylene system. The copolymer $(EO)_{19}(PO)_{43}(EO)_{19}$ (Pluronic P84) is of the same PEO content as $(EO)_{13}(PO)_{30}(EO)_{13}$ (Pluronic L64), of which the phase diagram with water and xylene

we have published earlier,[23] but has a 45% higher molecular weight.

The focus of this paper is the discovery and the ramifications of the richest structural polymorphism ever observed in amphiphile-containing mixtures: the $(EO)_{19}(PO)_{43}(EO)_{19}-{}^2H_2O-p$-xylene system exhibits nine different phases, all thermodynamically stable at the same temperature (25 °C). The presentation of our findings commences with the structural characterization of the lyotropic liquid crystalline phases, employing small-angle X-ray scattering (SAXS) as the primary tool. The different structures are analyzed/discussed in order of increasing complexity: lamellar, (normal and reverse) hexagonal, bicontinuous cubic, and micellar cubic; the bulk copolymer structure is also examined. An overview of the phase behavior follows, where the self-assembly of amphiphilic block copolymers and the factors influencing the evolution/progression of structure in the particular ternary PEO/PPO–water–oil phase diagram are discussed. Finally, we consider the notable formation of four different cubic structures.

Besides having important ramifications in practical applications (recall that PEO/PPO block copolymers are commercially available), our studies on the structural polymorphism in selective solvents establish amphiphilic PEO/PPO block copolymers as model systems, which can help clarify both the thermodynamics and the dynamics of self-assembly phenomena that are analogous to those in a wide range of synthetic and biological systems.

Materials and Methods

Materials. The Pluronic P84 poly(ethylene oxide)-*block*-poly-(propylene oxide)-*block*-poly(ethylene oxide) copolymer was obtained as a gift from BASF Corp. and was used as received. P84 can be represented by the formula $(EO)_{19}(PO)_{43}(EO)_{19}$ based on its nominal molecular weight of 4200 and 40% PEO content. ${}^2H_2O$ (99.80 atom % ${}^2H$) was purchased from Dr. Glaser AG, Basel, Switzerland. *p*-Xylene of purity >99.0% was obtained from Fluka Chemie AG, Buchs, Switzerland. Samples were prepared individually by weighing appropriate amounts of copolymer, water, and oil into 8 mm (i.d.) glass tubes which were immediately flame-sealed. The samples were centrifuged repeatedly in alternating directions over the course of several days to facilitate mixing (when viscous) and then in one direction to speed up phase separation (if not single-phase); the samples were kept at 25 ± 0.5 °C.

Determination of the Phase Boundaries. Following an equilibration period, the samples were checked for phase separation (one-phase samples were clear and macroscopically homogeneous; the two- or three-phase samples either were homogeneous but opaque or were macroscopically heterogeneous/phase-separated) and optical anisotropy (micellar solutions or cubic lyotropic liquid crystals are isotropic/nonbirefringent, while lamellar or hexagonal lyotropic liquid crystals are anisotropic/birefringent). Whether a certain sample consisted of a single homogeneous phase, or of two or three phases, was also established from ${}^2H$ NMR measurements (carried out at a resonance frequency of 15.371 MHz (2.3 T) on a Bruker MSL100 pulsed superconducting spectrometer working in the Fourier transform mode). The presence of an isotropic phase is directly noted from a sharp singlet in the ${}^2H$ NMR spectra and that of an anisotropic phase from a doublet of broad peaks.[22]

Structural Characterization Using Small-Angle X-ray Scattering (SAXS). SAXS measurements were performed on a Kratky compact small-angle system equipped with a position-sensitive detector (see ref 25 for details). The obtained Bragg diffraction peaks are relatively sharp in which case the correct peak position can be evaluated directly from the slit-smeared data.[22,23] The structure of the lyotropic liquid crystalline phases was determined from the relative positions of the SAXS diffraction peaks. For the lamellar (smectic) and hexagonal (cylindrical assemblies crystallized in a two-dimensional hexagonal lattice) structures, the position of the peaks should obey the relationships

(17) Chu, B.; Zhou, Z. *Surf. Sci. Ser.* **1996**, *60*, 67.
(18) Alexandridis, P. *Curr. Opin. Colloid Interface Sci.* **1997**, *2*, 478.
(19) Mortensen, K. *J. Phys.: Condens. Matter* **1996**, *8*, A103.
(20) Wanka, G.; Hoffmann, H.; Ulbricht, W. *Macromolecules* **1994**, *27*, 4145.
(21) Glatter, O.; Scherf, G.; Schillen, K.; Brown, W. *Macromolecules* **1994**, *27*, 6046.
(22) Alexandridis, P.; Zhou, D.; Khan, A. *Langmuir* **1996**, *12*, 2690.
(23) Alexandridis, P.; Olsson, U.; Lindman, B. *Macromolecules* **1995**, *28*, 7700.
(24) Alexandridis, P.; Olsson, U.; Lindman, B. *J. Phys. Chem.* **1996**, *100*, 280.
(25) Alexandridis, P.; Olsson, U.; Lindman, B. *Langmuir* **1997**, *13*, 23.
(26) Alexandridis, P.; Holmqvist, P.; Lindman, B. *Colloids Surf., A* **1997**, *129–130*, 3.
(27) Holmqvist, P.; Alexandridis, P.; Lindman, B. *Macromolecules* **1997**, *30*, 6788.
(28) Wu, G. W.; Liu, L. Z.; Buu, V. B.; Chu, B.; Schneider, D. K. *Physica A* **1996**, *231*, 73.

1:2:3:4 ... and 1:$\sqrt{3}$:2:$\sqrt{7}$:3 ..., respectively. The lattice parameters *d* (lamellar periodicity), and *a* (distance between the centers of adjacent cylinders), of the lamellar and hexagonal structures, respectively, were obtained from the position (q^*) of the first (and most intense) diffraction peak

$$\text{lamellar:} \quad q^* = \frac{2\pi}{d}, \qquad \text{hexagonal:} \quad q^* = \frac{4\pi}{a\sqrt{3}} \quad (1)$$

The thickness of the apolar domains, δ, in the lamellar structure, and the radius of the apolar [polar] domains, *R*, in the normal [reverse] hexagonal structures were calculated from the lattice parameters and the volume fraction, f [$1 - f$], of the apolar (PPO + xylene) [polar (PEO + water)] components in the ternary system (see refs 23−25 for more details on the definition of "polar" and "apolar" domains)

$$\text{lamellar:} \quad \delta = df, \qquad \text{hexagonal:} \quad R = a\left(\frac{\sqrt{3}}{2\pi} f\right)^{1/2} \quad (2)$$

In the lamellar structure, the effective area per PEO block at the interface between polar and apolar domains (interfacial area, α_p) was determined from the lattice parameters without any assumptions concerning the degree of segregation or the local structure of the copolymer film.[25] The calculation of α_p in the normal [reverse] hexagonal structure also involved the apolar [polar] volume fractions (v_p is the volume of one copolymer molecule, $v_p \approx 6660$ Å³ for P84, and Φ_p is the copolymer volume fraction in the ternary system).

$$\text{lamellar:} \quad \alpha_p = \frac{v_p}{d\Phi_p}, \qquad \text{hexagonal:} \quad \alpha_p = \frac{v_p}{a\Phi_p}\left(\frac{2\pi}{\sqrt{3}} f\right)^{1/2} \quad (3)$$

The assessment of the crystallographic space group of the cubic structures was based on the relative positions of the SAXS diffraction peaks as well as their relative intensity.[22,25] The indexing of the SAXS peaks to different crystallographic space groups was assessed by plotting the reciprocal spacings ($1/d_{hkl}$) of the various reflections versus $m = (h^2 + k^2 + l^2)^{1/2}$ (where *h*, *k*, and *l* are the Miller indices). For a valid assignment, such a plot should pass through the origin and be linear with a slope of $1/a$, where *a* is the cubic cell lattice parameter. A proper crystallographic indexation of the lyotropic liquid crystalline cubic structures is often hindered by the small number of reflections obtained from such samples; information obtained from other structures in the phase diagram can prove beneficial in this case.[23−25] In the normal [reverse] micellar cubic structure, the lattice parameter (*a*) can be related to the copolymer volume per molecule (v_p), interfacial area (α_p), and the copolymer and apolar [polar] volume fractions (Φ_p and f [$1 - f$]) through simple geometrical arguments for the volume occupied by the *N* micelles which make up the unit cubic cell:

$$a = (36\pi N f^2)^{1/3} \frac{v_p}{2\Phi_p \alpha_p} \quad (4)$$

Agreement between the α_p values thus obtained for a given *N* (which depends on the crystallographic space group) and the α_p values in the (adjacent to the normal [reverse] micellar cubic) normal [reverse] hexagonal structure is indicative of the use of a correct *N* and space group. In the bicontinuous cubic structures, the identification of the crystallographic group from the SAXS peak assignment can be confirmed by comparing the α_p values in the (adjacent to the normal [reverse] bicontinuous cubic) normal [reverse] hexagonal and lamellar structures to the α_p values obtained from an analysis of the bicontinuous interfacial region described in terms of minimal surfaces of different crystallographic groups.[23−25,29]

(29) Anderson, D.; Wennerström, H.; Olsson, U. *J. Phys. Chem.* **1989**, *93*, 4243.

Structural Characterization of the Lyotropic Mesophases

Lamellar Structure (L$_\alpha$). L$_\alpha$ is the most extensive of the liquid crystalline phases. It forms on the binary (EO)$_{19}$-(PO)$_{43}$(EO)$_{19}$−water axis at 67−87 wt % copolymer and can accommodate up to 25 wt % xylene, much more than the oil-in-water (normal) L$_1$, I$_1$, and H$_1$ phases (see Figures 1 and 11). The one-dimensional lamellar (smectic) structure (shown schematically in Figure 1) of the samples in the L$_\alpha$ region has been established by SAXS measurements that gave diffraction patterns with second- and even third-order peaks obeying the 1:2:3 relationship (see Figure 2). Values for the lamellar lattice periodicity (spacing), *d*, the apolar (PPO + xylene) thickness, δ, and the interfacial area per PEO block, α_p, are plotted in Figure 3 as a function of the copolymer volume fraction. The *d* values decreased from 136 to 82 Å with increasing copolymer volume fraction from 0.4 to 0.8; as the copolymer concentration increases, the amount of interface (and lamellae) increases and thus the spacing between the lamellae decreases. The apolar thickness increased to a limited extent with increasing copolymer (and PPO) concentration at constant oil content but decreased considerably with increasing copolymer concentration at constant water content; in this case the increase in PPO content is not sufficient to compensate for the corresponding decrease in the oil content. The δ values are in the range 40−65 Å. The α_p values in the L$_\alpha$ region are in the range 100−125 Å² and decrease (by about 20%) with increasing copolymer concentration.

Hexagonal Structures (Normal, H$_1$, and Reverse, H$_2$). The H$_1$ region is stable in the 44−61 wt % copolymer range along the binary (EO)$_{19}$(PO)$_{43}$(EO)$_{19}$−water axis and swells with up to 7 wt % xylene (Figure 1). The two-dimensional hexagonal structure (consisting of cylindrical self-assemblies crystallized in an hexagonal lattice as shown schematically in Figure 1) of samples in the H$_1$ region was established by SAXS experiments (the relative positions of the four peaks resolved in the diffraction pattern of Figure 4a correspond to the 1:$\sqrt{3}$:2:$\sqrt{7}$ relationship), while the normal (oil-in-water) morphology was ascertained from the location of the H$_1$ region in the ternary phase diagram along the copolymer−water axis. The nearest neighbor (cylinder) distance decreased with increasing copolymer content from 121 Å at 40.0/57.5/2.5 wt % to 118 Å at 50.0/47.5/2.5 wt % copolymer/water/oil, consistent with a denser packing of the cylinders as their number increased. The interfacial area per PEO block was 121−125 Å², similar to that in the lamellar phase at copolymer concentrations comparable to those of the H$_1$ region.

The H$_2$ region extends in the 36−78 wt % copolymer range and 9−21 wt % water range. A SAXS diffraction pattern from a H$_2$ sample is presented in Figure 4b; the 1:$\sqrt{3}$:2:$\sqrt{7}$:3:$\sqrt{12}$ relative position of the six Bragg peaks observed confirmed the two-dimensional hexagonal structure (shown schematically in Figure 1). The reverse (water-in-oil) morphology can be ascertained from the location of the H$_2$ region in the ternary phase diagram, between the L$_\alpha$ and L$_2$ phases. Characteristic structural parameters for samples spanning the reverse hexagonal region are plotted in Figure 5 as a function of the copolymer volume fraction. The distance between the centers of two adjacent cylinders decreased (from 155 to 111 Å) with increasing copolymer volume fraction (from 0.37 to 0.68); the polar (PEO + water) cylinder radius, *R*, also decreased (from 46 to 36 Å). The dependence on copolymer concentration of two other lengths, *b* and *c*, characteristic to the hexagonal structure is shown in Figure 5b. $b = a - $
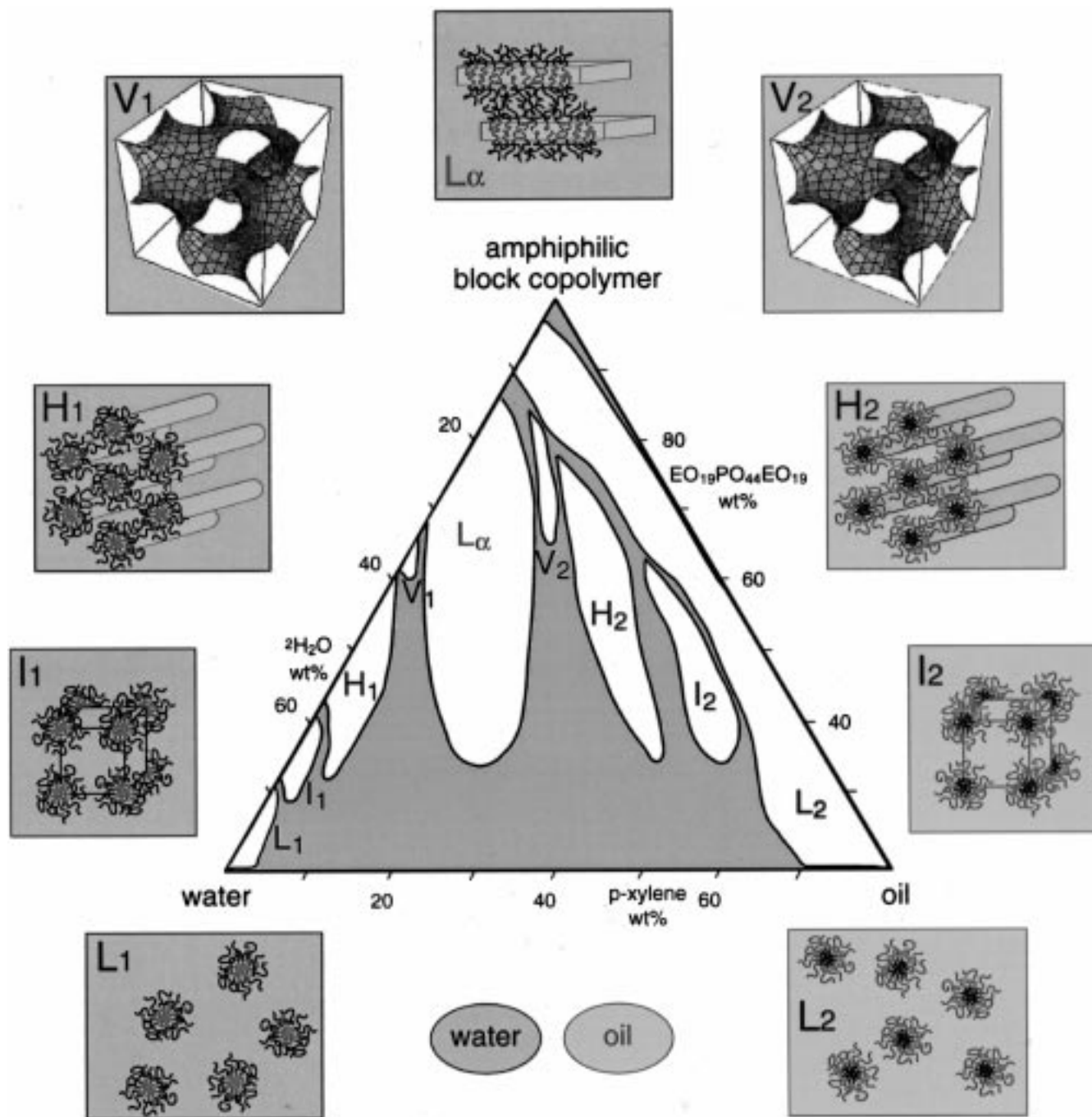
Figure 1. Phase diagram of the $(EO)_{19}(PO)_{43}(EO)_{19}-{}^{2}H_2O$ ("water")$-p$-xylene ("oil") ternary system at 25 °C. The phase boundaries of the one-phase regions are drawn with solid lines. I_1, H_1, V_1, L_α, V_2, H_2, and I_2, denote normal (oil-in-water) micellar cubic, normal hexagonal, normal bicontinuous cubic, lamellar, reverse (water-in-oil) bicontinuous cubic, reverse hexagonal, and reverse micellar cubic lyotropic liquid crystalline phases, respectively, while L_1 and L_2 denote water-rich (normal micellar) and water-lean/oil-rich (reverse micellar) solutions. The concentrations are expressed in wt %. The samples whose compositions fall outside the one-phase regions are dispersions of two or three (depending on the location in the phase diagram) different phases. The line along the copolymer−oil axis indicates incomplete miscibility between the copolymer and the oil. Schematics of the different modes of self-organization of the amphiphilic block copolymers in the presence of solvents ("water" and "oil") are shown adjacent to the respective phases in the phase diagram. The amphiphiles are localized at the interfaces between the water and oil domains (denoted by light blue and red colors, respectively). The *Ia3d*/Gyroid minimal surface is used as a representation of the microstructure in the V_1 and V_2 phases.

$2R$, is the shortest distance between nearest-neighbor polar/apolar interfaces and corresponds to the smallest thickness of two overlapping (and interacting) PPO layers, while $c = b + R(2/\sqrt{3} - 1)$ is the normal distance from the polar/apolar interface to the center of the triangular interstice (see the inset of Figure 5b). Both b and c decrease significantly (from ≈70 to ≈40 Å) with increasing copolymer volume fraction, indicating a denser packing

of the PPO chains. The lowest value of b found in the H_2 region (at high copolymer and low oil contents) is ≈40, comparable to the δ values in the L_α region in the absence of oil.

Bicontinuous Cubic Structures (Normal, V_1, and Reverse, V_2). The V_1 region occurs along the binary $(EO)_{19}(PO)_{43}(EO)_{19}$−water axis at 62−66 wt % copolymer concentration and has limited ability to swell with oil.
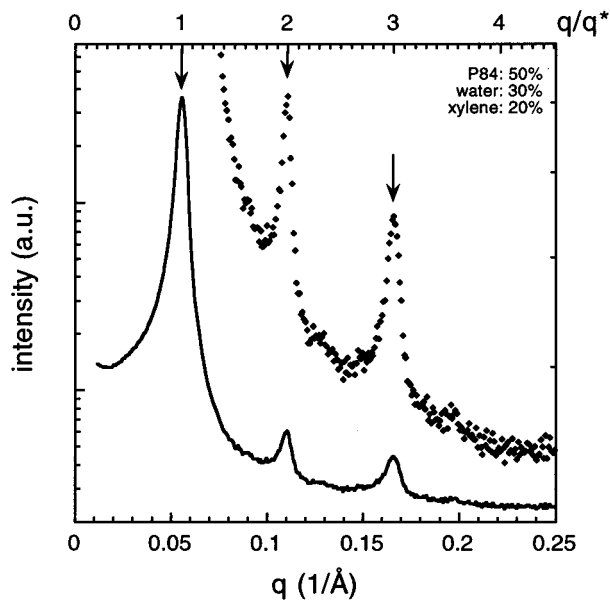
Figure 2. SAXS diffraction pattern obtained from a lamellar, L_α, liquid crystalline sample of 50.0/30.0/20.0 copolymer/water/oil wt % composition at 25 °C. The scattering curve is also shown on an expanded intensity scale to expose the higher order Bragg peaks (marked with the arrows). The positions of the higher order reflections with respect to that of the first (and most intense) peak, q^*, are indicated on the upper *X*-axis.

The samples in this region are isotropic (nonbirefringent) and very stiff, characteristics of cubic structure; the location of V_1 in the phase diagram (between the H_1 and L_α phases) indicates that its structure is bicontinuous with the curvature of the polar/apolar interface toward oil.[30] This is the first time a normal bicontinuous phase has been observed in PEO/PPO block copolymer–water systems. Two complementary descriptions are often used for bicontinuous cubic phases in surfactant systems, (i) that of a multiply connected bilayer (described in terms of minimal surfaces of cubic symmetry) separating two distinguishable and continuous domains of the same solvent and (ii) that of two infinite channel networks of interconnected cylinders (associated with the skeletal graphs of the two interwoven subvolumes separated by the minimal dividing surface of the bilayer description).[25,30] We can thus visualize the microstructure in the V_1 region to be that of a polar film consisting of PEO and water which forms a dividing bilayer between two apolar domains containing PPO and xylene (as seen in Figure 10a of ref 25). Since the two apolar domains are not connected to each other, this structure can also be called tricontinuous (one polar domain and two apolar ones).

The narrow (with respect to water–oil range) V_2 region occurs between the L_α and H_2 phases at high (67–84 wt %) copolymer concentration and has the same macroscopic appearance as V_1. The relative position of this cubic phase in the phase diagram (between the L_α and H_2 phases) indicates that its structure is bicontinuous with the curvature of the polar/apolar interface toward water.[30] A V_2 bicontinuous cubic region is also present in the $(EO)_{13}$-$(PO)_{30}(EO)_{13}$-^2H_2O-*p*-xylene phase diagram.[23] From the expected curvature of the polar/apolar interface, we anticipate the molecular arrangement in the V_2 region to be that of an apolar film consisting of PPO and oil which forms a dividing bilayer between two polar domains containing PEO and water (and thus call V_2 reverse or water-in-oil).
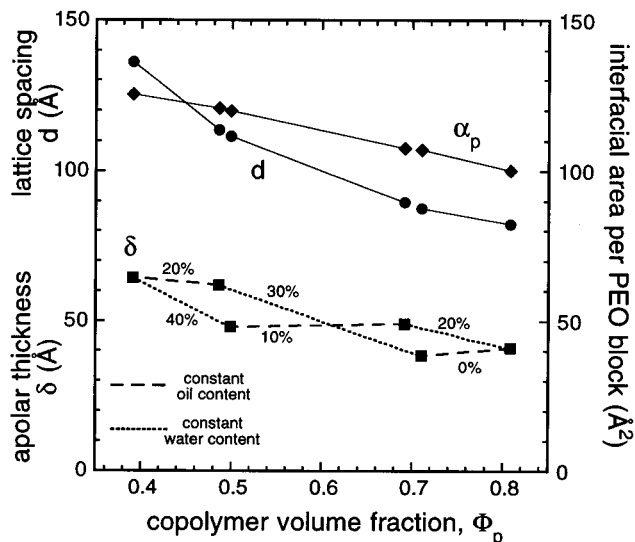

Figure 3. Characteristic structural parameters (lattice spacing, apolar film thickness, and interfacial area per PEO block) in the lamellar, L_α, liquid crystalline region, plotted as a function of the copolymer volume fraction at constant (0, 10, and 20 wt %) oil content, and at constant (20, 30, and 40 wt %) water content.

SAXS diffraction patterns obtained from samples in the V_1 and V_2 regions are shown in Figure 6. The two patterns are strikingly similar, with the scattering function in parts a and b of Figure 6 dominated by a strong correlation peak at $q = 0.0691$ and $q = 0.0686$ Å^{-1}, respectively. The most commonly observed space group of bicontinuous cubic phases in surfactant and lipid systems is $Ia3d$ (Q^{230}),[30,31] where the bilayer/channel structure can be associated with the so-called Gyroid (G) minimal surface. This space group allows the Bragg reflections $hkl = 211, 220, 321, 400, 420, 332, 422, ...$, which give peaks in the relative (scattering vector) positions $\sqrt{6}$, $2\sqrt{2}$, $\sqrt{14}$, 4, $\sqrt{20}$, $\sqrt{22}$, $2\sqrt{6}$, ..., of which the first reflection, corresponding to $hkl = 211$, is the most intense.[31] The second well-defined reflection in the diffraction patterns of Figure 6 follows the sequence $1:2/\sqrt{3}$ (=1.155) (with respect to the first peak) and is hence consistent with the 220 reflection of the $Ia3d$ space group; a number of other (weak) peaks are marked in the SAXS diffraction pattern of Figure 6 with filled arrows and can be identified as the higher order (222, 321, 400, 420, 332, and 422) reflections of the $Ia3d$ structure. The hump seen in the scattering pattern of Figure 6a at $q \approx 0.035$ Å^{-1} may be an indication of some type of higher order organization (it occurs at $q \approx 0.035$ Å^{-1}, half of the q value of the main correlation peak). This identification of the $Ia3d$/Gyroid structure in the V_1 and V_2 regions of the $(EO)_{19}(PO)_{43}(EO)_{19}$–water–oil phase diagram receives further support when we calculate the area of the polar/apolar interface using the parallel surface model for the Gyroid surface.[24,25,29] The area per copolymer molecule thus obtained is very similar to that found in L_α samples adjacent to the V_1 and V_2 phases. From the $1/d_{hkl}$ vs $m = (h^2 + k^2 + l^2)^{1/2}$ plots shown in Figure 7 (based on the positions of the peaks marked in Figure 6), we obtained cell lattice parameter values of $a = 247$ and 221 Å, for the V_1 and V_2 structures, respectively.

Micellar Cubic Structures (Normal, I_1, and Reverse, I_2). The I_1 region is stable along the binary $(EO)_{19}$-$(PO)_{43}(EO)_{19}$–water axis in the 33–42 wt % copolymer concentration range (see Figure 1). The samples in this

(30) Fontell, K. *Colloid Polym. Sci.* **1990**, *268*, 264.

(31) Lindblom, G.; Rilfors, L. *Biochim. Biophys. Acta* **1989**, *988*, 221.
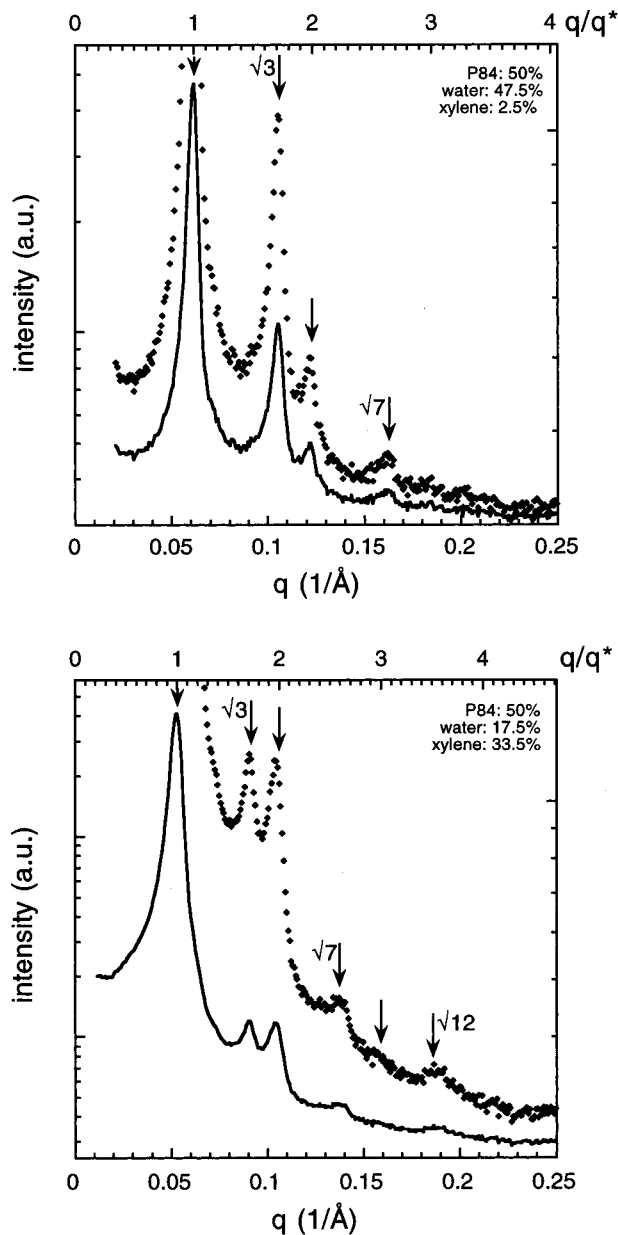
Figure 4. SAXS diffraction patterns obtained from (a, top) normal hexagonal, H_1, and (b, bottom) reverse hexagonal, H_2, liquid crystalline samples of 50.0/47.5/2.5 and 50.0/17.5/33.5 wt % copolymer/water/oil compositions, respectively, at 25 °C. The scattering curves are also shown on an expanded intensity scale to reveal the higher order $\sqrt{3}$, 2, $\sqrt{7}$, 3, and $\sqrt{12}$ Bragg peaks. The positions of the higher order reflections with respect to that of the first (and most intense) peak, q^*, are indicated on the upper X-axis of each graph.

region are stiff and nonbirefringent, characteristics of a cubic liquid crystalline structure. The location of this cubic phase in the ternary phase diagram (between the aqueous micellar solution and the normal hexagonal phase) suggests[30] that its microstructure consists of normal micelles which have crystallized into a cubic lattice (as shown schematically in Figure 1). The formation by PEO−PPO−PEO copolymers (of sufficiently high PEO content and molecular weight—note that $(EO)_{13}(PO)_{30}(EO)_{13}$ does not form an I_1 phase[22,23]) in aqueous solutions of "gels" (as the normal micellar cubic regions are often called in the applications' literature) has been known[10] and utilized[10,13,14] for years; however the cubic structure has only lately been characterized by small-angle neutron scat-
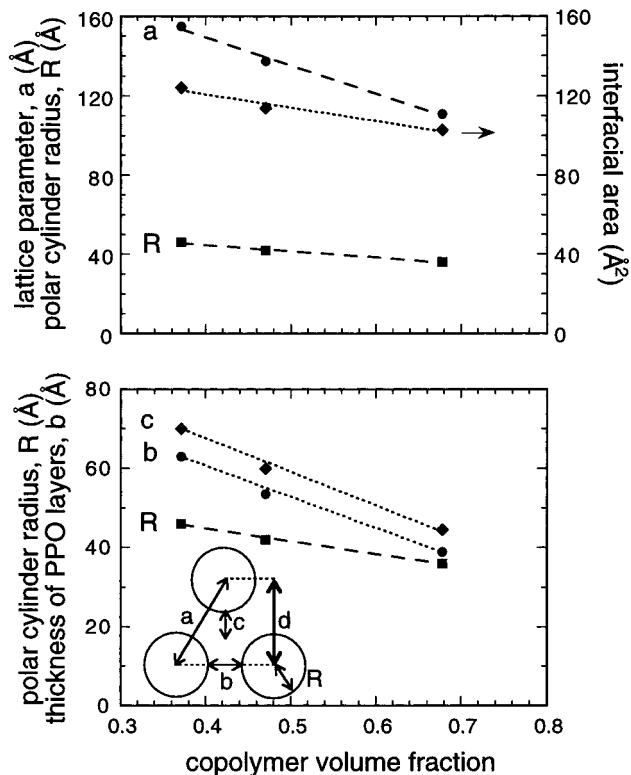
Figure 5. (a, top) Characteristic structural parameters (lattice parameter/nearest neighbor distance, polar cylinder radius, and interfacial area per PEO block) in the reverse hexagonal, H_2, region, plotted as a function of the copolymer volume fraction (the sample compositions are 70.0/12.5/17.5, 50.0/17.5/32.5, and 40.0/20.0/40.0 wt % copolymer/water/oil). (b, bottom) The shortest distance between nearest-neighbor polar/apolar interfaces, b, and the normal distance from the polar/apolar interface to the center of the triangular interstice, c, plotted together with the polar cylinder radius, R, as a function of the copolymer volume fraction. A triangular section of the hexagonal structure is included in the graph to illustrate the various characteristic lengths.
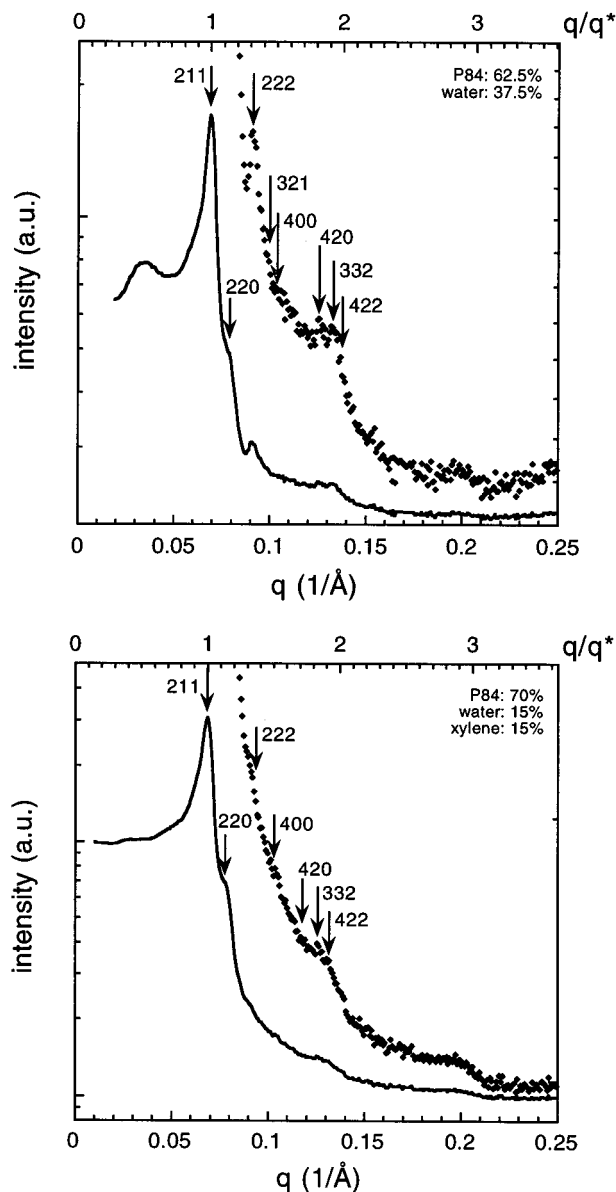
tering (SANS)[19,32] and SAXS.[22,33] The latter usually allows much better resolution of the numerous reflections originating from the cubic structure.[22,33]

A SAXS diffraction pattern obtained from a I_1 sample is presented in Figure 8a. A total of five Bragg peaks are identified (marked with arrows), which can be indexed as the $hkl = 110, 200, 211, 220,$ and 310 reflections of a body-centered (I...) close-packed cubic structure, characterized by Bragg reflections whose reciprocal d spacings follow the relationship $\sqrt{2}:\sqrt{4}:\sqrt{6}:\sqrt{8}:\sqrt{10}$ .... The relative intensity of the observed peaks (as well as the very low intensity of the 310 reflection, and the inability to discern higher order reflections) follow the trend expected from structures of cubic aspect 8 and, more specifically, from the centrosymmetric $Im3m$ (Q^{229}) space group.[34] The straight line passing through the origin of the $1/d_{hkl}$ versus $m = (h^2 + k^2 + l^2)^{1/2}$ plot shown in Figure 9a indicates the good fit of the data to the $Im3m$ structure. The value of the cubic cell lattice parameter, a, was estimated at 139 Å from the slope of the plot of Figure 9a. A lattice parameter of 158 Å was obtained using simple geometrical arguments for the volume occupied by the (N=) two normal micelles which make up the unit cell of the I... structure,

(32) Prud'homme, R. K.; Wu, G., Schneider, D. K. *Langmuir* **1996**, *12*, 4651.
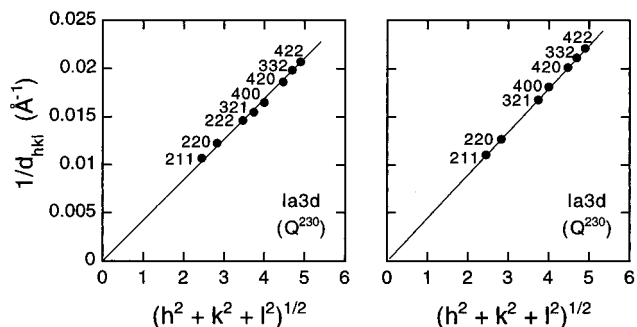(33) Diat, O.; Porte, G.; Berret, J.-F. *Phys. Rev. B* **1996**, *54*, 14869.
(34) Mariani, P.; Luzzati, V.; Delacroix, H. *J. Mol. Biol.* **1988**, *204*, 165.

Figure 7. Plots of the reciprocal *d* spacings ($1/d_{hkl}$) of the reflections marked in the SAXS diffraction pattern of (a, left) Figure 6a, and (b, right) Figure 6b plotted versus $m = (h^2 + k^2 + l^2)^{1/2}$. The linearity of the plots and the (0,0) intercept are indications of a valid crystallographic space group assignment. The cubic cell lattice parameters obtained from the slope of the plots are (a) 247 Å and (b) 221 Å.

as a subset the ones from the higher symmetry I... structure) could be discerned in the diffraction patterns obtained from I_1 samples.

The I_2 region occurs between the L_2 and H_2 regions at 36–64 wt % copolymer and 6–12 wt % water contents, as seen in Figures 1 and 11b. The I_2 samples are transparent, nonbirefringent, and stiff, features characteristics of a cubic organization. The location of this cubic phase in the ternary phase diagram suggests[25,30] that its microstructure consists of reverse micelles which have crystallized into a cubic lattice (as shown schematically in Figure 1). As we discuss in more detail below, this is one of the first times such a structure has been observed in amphiphile–water–oil systems (and the first time it is reported for a PEO–PPO–PEO copolymer system), and the ability of the $(EO)_{19}(PO)_{43}(EO)_{19}$ reverse micelles to crystallize can provide insight on the intermicellar interactions.

The SAXS diffraction pattern obtained from a I_2 sample is presented in Figure 8b. A total of nine Bragg peaks were resolved (marked with arrows), which can be indexed as the 111, 220, 222, 331, 422, 333, 442, 533, and 551/711 reflections of the face-centered cubic space group $Fd3m$ (Q^{227}).[35,36] A proposed structural model for the $Fd3m$ cubic phases involves a total of 24 spherical micelles per unit cell, with a bimodal size distribution composed of 8 larger and 16 smaller micelles.[35] A lattice parameter of $a = 347$ Å was obtained from plotting the reciprocal *d* spacings ($1/d_{hkl}$) of the nine observed reflections versus *m* (Figure 9b). From a calculation of the volume occupied by the ($N=$) 24 reverse micelles which participate in a $Fd3m$ cubic unit cell ($\Phi_p = 0.362$ and $1 - f = 0.224$ for the 50.0/10.0/40.0 wt % copolymer/water/oil composition), a lattice parameter of 378 Å was obtained, consistent (only 9% higher) with the lattice parameter determined from the SAXS data in the context of the $Fd3m$ structure, and thus in support of the $Fd3m$ structure.

Water-Rich and Water-Lean Solution (Normal Micellar, L_1, and Reverse Micellar, L_2). In addition to the phases of liquid crystalline microstructure which occupy the major part of the $(EO)_{19}(PO)_{43}(EO)_{19}-{}^2H_2O-$ *p*-xylene phase diagram (above 35 wt % copolymer), two isotropic solution regions, L_1 and L_2, are present in the water-rich corner and the water-lean side, respectively, of the phase diagram. At concentrations below 2.5 wt %

Figure 6. SAXS diffraction patterns obtained from (a, top) normal bicontinuous cubic, V_1, and (b, bottom) reverse bicontinuous cubic, V_2, liquid crystalline samples of 62.5/37.5/0.0 and 70.0/15.0/15.0 wt % copolymer/water/oil compositions, respectively, at 25 °C. The scattering curves are also shown on an expanded intensity scale to reveal the higher order Bragg peaks. The arrows mark the positions of the observed reflections which match to reflections afforded by the $Ia3d$ crystallographic space group. The positions of the higher order reflections with respect to that of the first (and most intense) peak, q^*, are indicated on the upper *X*-axis.

and taking into account the values of Φ_p (=0.412) and *f*(=0.255) for the 40.0/60.0/0.0 copolymer/water/oil wt % sample composition and the interfacial area per PEO block (assumed to be 125 Å^2 as in the neighboring H_1 samples). The consistency (13% difference) of this predicted lattice parameter value with the experimentally determined one provides further evidence in support of the characterization of the normal micellar cubic structure as body-centered. We note here that the lattice parameter expected for a primitive P... cubic cell ($N = 1$), estimated from the same geometrical arguments used above, is 126 Å. This value is also consistent (9% difference) with that obtained from Figure 9a and would make a P... assignment plausible; however no reflections characteristic only of P... (the reflections afforded by the P... structure include

(35) Luzzati, V.; Vargas, R.; Gulik, A.; Mariani, P.; Seddon, J. M.; Rivas, E. *Biochemistry* **1992**, *31*, 279.
(36) Alexandridis, P.; Olsson, U.; Lindman, B. *Langmuir* **1996**, *12*, 1419.
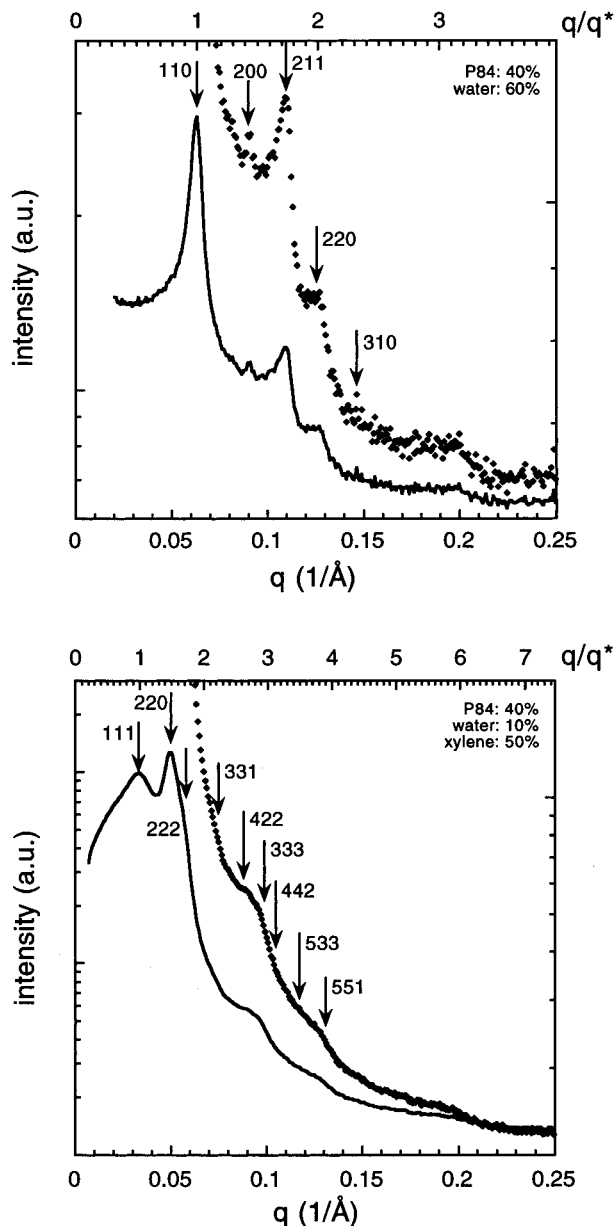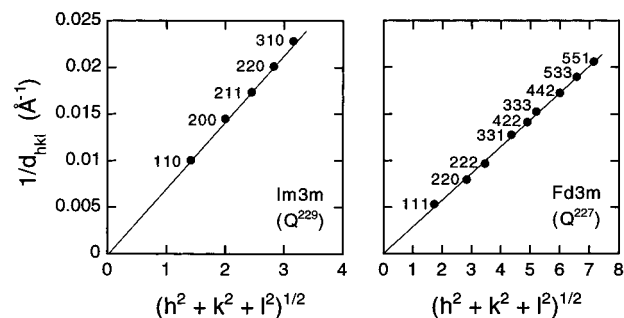
Figure 8. SAXS diffraction patterns obtained from (a, top) normal micellar cubic, I_1, and (b, bottom) reverse micellar cubic, I_2, liquid crystalline samples of 40.0/60.0/0.0 and 40.0/10.0/50.0 wt % copolymer/water/oil compositions, respectively, at 25 °C. The scattering curves are also shown on an expanded intensity scale to reveal the higher order Bragg peaks. The arrows mark the positions of the observed reflections which match to reflections afforded by the *Im3m* (a) and *Fd3m* (b) crystallographic space groups. The positions of the higher order reflections with respect to that of the first peak, q^*, are indicated on the upper X-axis.

(at 25 °C), the $(EO)_{19}(PO)_{43}(EO)_{19}$ molecules are dissolved in water as individual polymer chains (unimers).[37] At higher concentrations (and temperatures), they self-assemble into micelles which have the ability to solubilize hydrophobic compounds in their PPO core;[38] the L_1 region can thus extend up to ≈3 wt % xylene. Micelles (of the reverse, water-in-oil, type) are also present in a major part of the L_2 region.[39,40] $(EO)_{19}(PO)_{43}(EO)_{19}$ is unable to

(37) Alexandridis, P.; Holzwarth, J. F.; Hatton, T. A. *Macromolecules* **1994**, *27*, 2414.
(38) Hurter, P. N.; Alexandridis, P.; Hatton, T. A. *Surf. Sci. Ser.* **1995**, *55*, 191.
(39) Chu, B. *Langmuir* **1995**, *11*, 414.

Figure 9. Plots of the reciprocal *d* spacings ($1/d_{hkl}$) of the reflections marked in the SAXS diffraction pattern of (a, left) Figure 8a, and (b, right) Figure 8b plotted versus $m = (h^2 + k^2 + l^2)^{1/2}$. The linearity of the plots and the (0,0) intercept are indications of a valid crystallographic space group assignment. The cubic cell lattice parameters obtained from the slope of the plots are (a) 139 Å and (b) 347 Å.
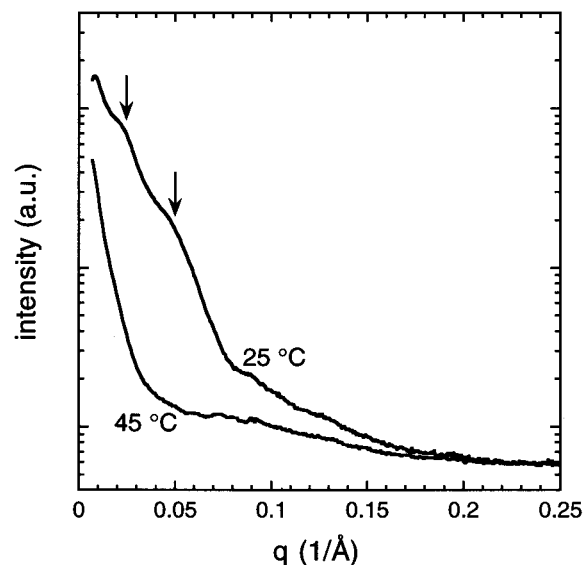
Figure 10. SAXS diffraction patterns obtained from bulk (as received) $(EO)_{19}(PO)_{43}(EO)_{19}$ (Pluronic P84) at 25 and 45 °C (the two scattering curves are drawn on the same scale). The difference between the two patterns is indicative of an order−disorder transition related to the melting of PEO crystalline domains.

form reverse micelles and accommodate significant amounts of water at copolymer concentrations less that ≈15 wt %;[40] for micelles to form, the presence of some water (≈0.15 water molecules per EO segment[39]) is also required. The maximum amount of water taken up by the reverse micelles corresponds to about 2.6 water molecules per EO segment. A SANS study on the structural characterization of the $(EO)_{19}(PO)_{43}(EO)_{19}$ reverse micelles has been carried out in our laboratory and will be reported elsewhere.

Dry PEO/PPO Block Copolymer (No Solvent Added). As alluded to in the introduction, some PEO/PPO block copolymers have been reported to exhibit structure in the absence of solvent.[11,12] We employed SAXS in order to check for structure in the case of solvent-free $(EO)_{19}(PO)_{43}(EO)_{19}$ (no solvent was added, but some water may have been present). At room temperature, the $(EO)_{19}$-$(PO)_{43}(EO)_{19}$ copolymer has an opaque appearance, indicative of the presence of domains having size larger than the visible wavelength. The diffraction pattern at 25 °C,

(40) Alexandridis, P.; Andersson, K. *J. Phys. Chem. B* **1997**, *101*, 8103.

reported in Figure 10, shows a high intensity at low q values (which is the counterpart of the optical scattering) but also reveals two humps at $q \approx 0.025$ Å^{-1} and $q \approx 0.050$ Å^{-1}. These humps, along with the high scattering at low q values, disappear when the copolymer is heated to 45 °C (see lower curve in Figure 10).

The q values for the two humps at 25 °C follow the 1:2 order and indicate a lamellar mesophase with (crystalline) PEO-rich and (amorphous) PPO-rich domains, consistent with previous reports for solvent-free triblock[12] PEO−PPO−PEO and diblock[11] PEO−PPO copolymers. The lamellar spacing corresponding to $q \approx 0.025$ Å^{-1} is approximately 250 Å, much larger than the copolymer radius of gyration ($\approx$17 Å[12]). This suggests that the whole chain is in an extended conformation; PEO crystallizes in a helical conformation (as judged by wide-angle X-ray measurements), while PPO crystallizes in a transplannar (tilted with respect to the lamellar end-plane) conformation.[11] The crystalline PEO melts at about 40 °C,[12] and the scattering pattern of $(EO)_{19}(PO)_{43}(EO)_{19}$ at 45 °C shows no correlation peak, indicating no significant segregation in the melted state.

Amphiphilic Block Copolymer−Water−Oil Phase Behavior: A New Paradigm in Self-Assembly

Overview of the $(EO)_{19}(PO)_{43}(EO)_{19}-{}^2H_2O-p$-Xylene Ternary Phase Diagram. The isothermal phase diagram obtained at 25 °C for the ternary system $(EO)_{19}$-$(PO)_{43}(EO)_{19}-{}^2H_2O-p$-xylene is presented in Figure 1. A record number of nine different phases are present in this phase diagram. Seven different lyotropic liquid crystalline phases have been identified (in terms of location in the phase diagram) and characterized (in terms of microstructure—see previous section for details): lamellar (L_α), normal (H_1) and reverse hexagonal (H_2), normal (V_1) and reverse bicontinuous cubic (V_2), and normal (I_1) and reverse micellar cubic (I_2). Two isotropic solution phases, one (normal micellar) rich in water (L_1) and one with high xylene-to-water ratio (L_2), have also been identified. The total will be 10 phases if we also consider the solvent-free $(EO)_{19}(PO)_{43}(EO)_{19}$ which is in a lamellar state. The different modes of self-organization of the amphiphilic block copolymers in the presence of water and oil are illustrated in the schematics of Figure 1.

The phase boundaries of the one-phase regions are drawn in Figure 1 with solid lines. The samples whose compositions fall outside the one-phase regions are dispersions of two or three (depending on the location in the phase diagram) different phases.[23] While important for the study of phase behavior,[4] the tie-lines in the two-phase regions and the borders of the three-phase regions have not been thoroughly determined in the present $(EO)_{19}(PO)_{43}(EO)_{19}$ phase diagram (and are not shown in Figure 1); we rather focused our attention on the rich structural polymorphism of the one-phase regions. We present elsewhere information on tie-lines in two-phase regions and borders of the three-phase regions for PEO−PPO−PEO−water−oil systems comparable to that examined here.[23]

The phase diagram of Figure 1 confirms the trend (theoretically predicted for A−B block copolymer melts[8]) of increasing block segregation and tendency for self-organization with increasing copolymer molecular weight and establishes the validity of this trend in the case of PEO/PPO block copolymer self-assembly in selective solvents. The copolymer examined here, $(EO)_{19}(PO)_{43}$-$(EO)_{19}$ (Pluronic P84), has a 45% higher molecular weight than, but is of the same composition as $(EO)_{13}(PO)_{30}(EO)_{13}$

(Pluronic L64), whose phase diagram with water and xylene we have published earlier (see Figure 1 in ref 23). An increase in the composition stability range of the different structures, and also a formation of more types of lyotropic liquid crystalline structures) is observed with P84, as compared to L64. More details on the effects of copolymer molecular weight on the self-assembly of amphiphilic block copolymers (in the presence of selective solvents) will be presented elsewhere for a group of PEO/PPO block copolymers having the same block composition (40% PEO) and varying molecular weight.

Progression of Structure in the Ternary PEO/PPO−Water−Oil System. The relative location of the various phases in the PEO/PPO block copolymer−water−oil phase diagram follows the sequence $L_1 \rightarrow I_1 \rightarrow H_1 \rightarrow V_1 \rightarrow L_\alpha \rightarrow V_2 \rightarrow H_2 \rightarrow I_2 \rightarrow L_2$ (clockwise, starting from the water-rich corner of the ternary phase diagram of Figure 1). This phase/structure sequence is consistent with a decreasing interfacial mean curvature (H) from the left ($H > 0$) to the right ($H < 0$), with $H = 0$ in the lamellar phase.[30] We have attributed this modulation of the interfacial curvature (and the resulting structure) to the ability of the macromolecular blocks to swell with solvent to a varying extent depending on the amount of solvent(s) available.[23−26] For a PEO/PPO block copolymer of a given block composition and molecular weight, the types of structures obtained in the presence of selective (water and oil) solvents appear to be a function of the volume fraction of the polar (PEO + water)/apolar (PPO + xylene) components (similarly to the structure variation observed[8] in A−B block copolymer melts, at temperatures below the order−disorder transition, upon changing the A/B block composition). However, both the water/oil ratio and the total copolymer content are important in order for certain phases to form.

The progression of structure in the phase diagram can be discussed at two levels, (i) at varying water/oil ratio and constant total copolymer content (along composition lines parallel to the basis of the phase triangle of Figure 1) and (ii) at increasing total copolymer content and constant copolymer/oil [copolymer/water] ratio (along dilution lines originating from the water [oil] corner of the phase triangle of Figure 1, or along composition lines parallel to the basis of the Figure 11a [11b] plot—more discussion on this follows). An example of structure progression for the case of varying the water/oil ratio is the phase sequence $I_1 \rightarrow H_1 \rightarrow L_\alpha \rightarrow H_2 \rightarrow I_2 \rightarrow L_2$, observed at $\approx$40 wt % copolymer; this follows the interfacial curvature ideas presented above but does not include the V_1 and V_2 phases. Higher (>65 wt %) copolymer concentrations are required for the V_1 and V_2 structures to form; at such copolymer concentrations the I_1 and I_2 structures are no longer stable (because the curvature is also affected by the polymer concentration—see below).

The progression of structure with increasing total copolymer content at the copolymer−water (oil-lean) and the copolymer−oil (water-lean) sides of the ternary phase diagram is shown in Figure 11, where the degree that the different phases/structures can accommodate oil [water] is plotted as a function of the copolymer weight fraction in water (Figure 11a) [oil (Figure 11b)]. In the oil-lean part of the phase diagram (at a constant copolymer/oil ratio), the $(EO)_{19}(PO)_{43}(EO)_{19}$ amphiphilic block copolymer self-assembles upon increase of its concentration (and the relative contribution of PPO to the ternary composition) into the following structures: $L_1 \rightarrow I_1 \rightarrow H_1 \rightarrow V_1 \rightarrow L_\alpha \rightarrow L_2$. Note that this sequence does not include any of the reverse liquid crystalline structures (V_2, H_2, I_2); the PPO content of the copolymer is such (40%) that it does not
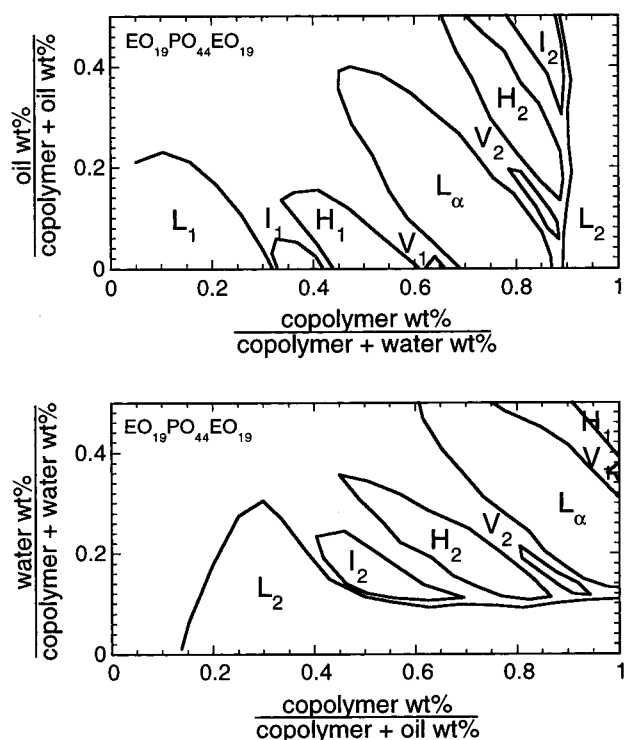
Figure 11. (a, top) Boundaries of the various phases along the copolymer−water side of the ternary phase diagram plotted in the "reduced" coordinates: X, copolymer weight fraction in its mixture with water; Y, oil weight fraction in its mixture with copolymer. (b, bottom) Boundaries of the various phases along the copolymer−oil side of the ternary phase diagram plotted in the "reduced" coordinates: X, copolymer weight fraction in its mixture with oil; Y, water weight fraction in its mixture with copolymer.

favor such structures in the absence of apolar solvent. The sphere → cylinder → plane sequence of structures, of the reverse (water-in-oil) morphology, is observed in the water-lean part of the phase diagram with increasing copolymer concentration (and increasing PEO volume fraction in the ternary copolymer−water−oil system) at a constant copolymer/water weight ratio (of about 1:4, corresponding to ≈1.4 water molecules per EO segment).

The decrease [increase] in the interfacial curvature (and the interrelated progression from a normal [reverse] spherical to a normal [reverse] cylindrical and then to a lamellar arrangement) upon an increase of the copolymer concentration at constant copolymer/oil [copolymer/water] ratio (Figure 11a [11b]) is a consequence of the relative increase of the PPO [PEO] block volume fraction in the system. The tilt to the left, observed in the phase boundaries as plotted in Figure 11, is a reflection of the curvature decrease [increase] upon the increase of the oil/water [water/oil] ratio. This resembles the observed increased swelling with water of the lyotropic phases in PEO/PPO copolymer−water systems upon increasing temperature, which has been interpreted in terms of decreasing effective interfacial curvature with increasing temperature (due to dehydration of the PEO block).[22]

Finally, we note that the different regions in the ternary phase diagram of Figure 1 are arranged symmetrically around the L_α region. The lack of "mirror image" symmetry in the present phase diagram is primarily due to the different nature of the PEO−water and the PPO− xylene interactions (see related discussion below). Differences in the conformational and volume-filling characteristics of each block, as well as fluctuation effects,

could also account for the lack of symmetry around the lamellar region, as discussed recently for diblock copolymer melts.[8]

Comparison with Other Self-Assembled Systems: Surfactant−Water−Oil Mixtures and Block Copolymer Melts. The self-assembly of amphiphilic block copolymers in the presence of selective solvents is related in some aspects to the self-assembly of surfactants in solution and in other aspects to the self-assembly of solvent-free block copolymers. It nevertheless exhibits a number of features which distinguish it from either surfactant or dry block copolymer self-assembly; we can thus consider the ternary phase behavior of the kind described in this paper as a new paradigm in self-assembly. The phase behavior of surfactants is influenced-limited by a "preferred" interfacial curvature (originating from the surfactant geometry) so that a ternary isothermal surfactant−oil−water phase diagram exhibits either normal (oil-in-water) or reverse (water-in-oil) phases, but usually not both.[1,41] In solvent-free block copolymers, the interfacial curvature is set by the relative composition of the different blocks.[8] A given block composition can typically result in only one type of structure; different relative block compositions are required for different structures to be formed. Homopolymers (A or B) can be used to modify the type of structure formed by A−B block copolymers.[42] In fact, recent modeling work[43] suggests that phase diagrams of ternary A−B block copolymer−A homopolymer−B homopolymer mixtures should exhibit the same general features as the ternary block copolymer− water−oil phase diagram presented here. To the best of our knowledge, no experimental A−B block copolymer−A homopolymer−B homopolymer phase diagram has been reported.

For amphiphilic block copolymers, the curvature is set initially by the relative length of the different blocks in the copolymer but can be readily tuned by the varying degree of swelling of the different blocks by the respective selective solvent. This extra degree of freedom is responsible for the unique structural polymorphism observed: both "normal" and "reverse" structures can be formed at the same temperature with the same block copolymer in the presence of two solvents selective for each block. We can conjecture from the above that the self-assembly of amphiphilic block copolymers in selective solvents is the (missing) link between the self-assembly of surfactants in water (and oil/cosurfactant) and the self-assembly of dry block copolymers. A recent report[44] of complex phase behavior in solvent-free nonionic "surfactants" failed to show whether the "surfactants" can self-assemble in the presence of selective solvents such as water.

Significance and Implications of the Micellar Cubic Phases. Besides the general features of the PEO/ PPO block copolymer phase behavior discussed above, the presence in the $(EO)_{19}(PO)_{43}(EO)_{19}$−water−$p$-xylene ternary system of four different cubic phases is unique and merits further consideration. There are four possible locations for the lyotropic cubic phases in a ternary amphiphile−water−oil phase diagram:[15,16,50] between the L_1 and H_1 or the L_2 and H_2 regions (where the cubic structure consists of close-packed normal or reverse

(41) Olsson, U. Wennerström, H. *Adv. Colloid Interface Sci.* **1994**, *49*, 113.

(42) Floudas, G.; Hadjichristidis, N.; Stamm, M.; Likhtman, A. E.; Semenov, A. N. *J. Chem. Phys.* **1997**, *106*, 3318.

(43) Janert, P. K.; Schick, M. *Macromolecules* **1997**, *30*, 137.

(44) Hillmyer, M. A.; Bates, F. S.; Almdal, K.; Mortensen, K.; Ryan, A. J.; Fairclough, J. P. A. *Science* **1996**, *271*, 976.

micellar, respectively), and between the L_α and the H_1 or H_2 regions (where the cubic structure is normal or reverse bicontinuous, respectively). The $(EO)_{19}(PO)_{43}(EO)_{19}$−water−$p$-xylene ternary system exhibits cubic phases in all four of the possible locations (i.e., normal micellar, I_1, normal bicontinuous, V_1, reverse bicontinuous, V_2, and reverse micellar, I_2). Four different cubic phases have been observed before in A−B block copolymer melts, but at different A/B block compositions and at different temperatures.[8] A few surfactant−water−oil systems are also known which exhibit structures of four with different crystallographic space groups within the same (e.g., bicontinuous) cubic region.[45] However, to the best of our knowledge, no ternary amphiphile−water−oil system has yet been reported with I_1, V_1, V_2, and I_2 phases.

In fact, as recently as 1990, no cubic phases had been identified[30,31] in amphiphile−solvent systems between the reverse micellar solution (L_2) and the reverse hexagonal (H_2) phase, presumably owing to the "low tendency [of reverse micelles] to organize in a regular manner".[30] Then came the report of a reverse cubic phase of probable crystallographic space group $Fd3m$, formed between the L_2 and H_2 regions of fully hydrated mixtures of phosphatidyl choline and diacylglycerol.[35,46] In 1996, we reported for the first time a reverse micellar cubic structure in a ternary amphiphilic block copolymer−water−xylene system.[36] The presence of the I_2 phase in the present $(EO)_{19}(PO)_{43}(EO)_{19}-{}^2H_2O-p$-xylene system (the first time I_2 is reported in PEO/PPO block copolymers—our previous I_2 report was for a PEO−poly(butylene oxide) copolymer) is thus unique and carries implications on the intermolecular and interassembly interactions of such amphiphiles.

High volume fractions of reverse micelles (corresponding to high amphiphile concentrations) would be required in order to make a crystalline packing possible, because of weak intermicellar interactions. Apparently, this is not easily achieved in the case of reverse micelles formed by typical (low molecular weight) surfactants. For the macromolecular amphiphile studied here, however, the micellar size and volume fraction and the interactions between reverse micelles are all sufficiently large to facilitate the micelle crystallization into a cubic array. The difficulty of forming reverse micellar cubic crystals (compared to the formation of normal micellar cubic crystals) is still reflected in the difference between the copolymer−water and copolymer−oil axes of the ternary phase diagram as depicted in Figure 11. Along the copolymer−water axis (Figure 11a), the copolymer content is the main determinant of the structures formed, while along the copolymer−oil axis (Figure 11b) a certain amount of water ($\approx$8 wt %) is required in addition to a sufficiently high copolymer content. The copolymer content at which the micellar cubic phases start forming is the same, about 35 wt %, for both the normal and the reverse cubic phase.

One might have expected (for symmetry reasons with respect to their position in the phase diagram) the normal and the reverse micellar cubic phases to have the same structure. The reason for the observed difference (I_1 is body-centered and I_2 is face-centered) is unclear but can possibly be attributed to the different interactions between the normal and reverse micelles.[47] The triblock sequence of the $(EO)_{19}(PO)_{43}(EO)_{19}$ copolymer should not be the reason for the different structures; diblock PEO−PBO[25]

and PEO−PPO (P. Alexandridis, unpublished results) copolymers also exhibit I_1 body-centered and I_2 face-centered structures. We note here that the polymer−solvent and polymer−polymer interactions (which we invoked above to explain the difference in structure between normal and reverse micellar cubic phases) also depend on the total copolymer content (and micelle volume fraction). Different crystallographic structures have been observed recently within the same (I_1) cubic region;[33] the concentration range covered by the cubic region of ref 33 was much greater than that of the I_1 and I_2 regions of the present system. The crystallographic structure can also be influenced by the sample shearing history.

Significance and Implications of the Bicontinuous Cubic Phases. The presence of two bicontinuous structures, one having the mean curvature of the polar/apolar interface toward oil (normal) and the other toward water (reverse), is another notable feature of the $(EO)_{19}(PO)_{43}$-$(EO)_{19}-{}^2H_2O-p$-xylene phase diagram. Bicontinuous cubic phases were first identified in surfactant−water and lipid−water systems in the 1960s.[31,48] The appeal of such phases increased when their microstructure was related to a geometrical description based on minimal surfaces.[48] Such complex structures hold intriguing implications in processes involving biological membranes (e.g., fusion)[31,48] and can be used as templates for, e.g., the synthesis (by polymerization of monomer-solvent or macromonomer-amphiphile) of porous membranes with well-defined structure and pore size[49] or the crystallization of (otherwise impossible to crystallize) membrane proteins.[50] We reported for the first time the formation of such structures in ternary amphiphilic (di- and tri-)block copolymer−water−oil systems.[23−25] Bicontinuous cubic phases of the $Ia3d$/Gyroid structure have also been observed in solvent-free diblock copolymers[8] and, most recently, in triblock copolymers.[51] The present report is the first time that a normal bicontinuous cubic phase has been identified (and properly characterized) in a binary PEO/PPO block copolymer−water system (our previous reports[23−25] have been for reverse bicontinuous cubic phases).

It is notable that the V_2 region borders on a copolymer-rich solution. This is reminiscent of the occurrence in diblock copolymer melts of bicontinuous cubic phases localized near the order−disorder transition (ODT); the stability of these phases has recently been related to fluctuation effects which become important in the vicinity of the ODT and favor isotropic (such as bicontinuous cubic) microstructures.[8] We have already related[23] the evolution of structure from the copolymer-rich (top) corner of the phase triangle (when we reported the first PEO/PPO block copolymer−water−oil phase diagram) to an ODT-like transition: "the pure [PEO/PPO block co]polymer can be considered as a disordered melt, whereupon structure and segregation are induced by the addition of water".

In block copolymer melts, structures other than bicontinuous cubic, most notably hexagonally perforated lamellae (HPL) or catenoid lamellae, have been reported, having curvature (and location in the phase diagram) intermediate to that of lamellar and (normal or reverse) hexago-

(45) Ström, P.; Anderson, D. M. *Langmuir* **1992**, *8*, 691.

(46) Orädd, G.; Lindblom, G.; Fontell, K.; Ljusberg-Wahren, H. *Biophys. J.* **1995**, *68*, 1856.

(47) Robbins, M. O.; Kremer, K.; Grest, G. S. *J. Chem. Phys.* **1988**, *88*, 3286.

(48) Hyde, S.; Andersson, S.; Larsson, K.; Blum, Z.; Landh, T.; Lidin, S.; Ninham, B. W. *The Language of Shape−The Role of Curvature in Condenced Matter, Physics, Chemistry and Biology*; Elsevier Science B.V.: Amsterdam, 1997.

(49) Lee, Y.-S.; Yang, J.-Y.; Sisson, T. M.; Frenkel, D. A. Gleeson, J. T.; Aksay, E.; Keller, S. L.; Gruner, S. M.; O'Brien, D. F. *J. Am. Chem. Soc.* **1995**, *117*, 5573.

(50) Pebay-Peyroula, E.; Rummel, G.; Rosenbusch, J. P.; Landau, E. M. *Science* **1997**, *277*, 1676.

(51) Avgeropoulos, A.; Dair, B. J.; Hadjichristidis, N.; Thomas, E. L. *Macromolecules* **1997**, *30*, 5634.

nal.[8,52] We have not observed such structures in the $(EO)_{19}(PO)_{43}(EO)_{19}-^2H_2O-p$-xylene system, either because we did not carry out scattering studies with well-oriented samples in different directions or because such structures are not thermodynamically stable in this system. In fact, there has been a concern about the thermodynamic stability of the HPL structures[53] (as well as of other structures observed in dry block copolymers[54]). This concern is compounded by the fact that the method of generating block copolymer phase diagrams involves cooling from a disordered state to an ordered state. Subject to a thermodynamic driving force, the polymer molecules must position themselves at the different microstructures while, at the same time, their mobility (already slow because they are macromolecules) slows down (because of decreasing temperature) and impedes the attainment of equilibrium. Indeed, very recent theoretical work[55,56] suggests that the HPL structures are not thermodynamically stable. We repeat here our belief that all the nine different structures reported in the present work are thermodynamically stable. The presence of the low-molecular weight solvents, the relatively low molecular weight of the block copolymer, and the sample preparation method we use, all contribute to this end.

Conclusions

A number of novel and significant contributions emerge from the present investigation on the phase behavior and structure of the $(EO)_{19}(PO)_{43}(EO)_{19}-^2H_2O-p$-xylene system (where water is a selective solvent for PEO and xylene a selective solvent for the PPO blocks): (i) the remarkable structural polymorphism afforded by this particular poly-(ethylene oxide)/poly(propylene oxide) (PEO/PPO) block copolymer (but also of PEO/PPO copolymers in general) in the presence of selective solvents, (ii) the relevance/connection of the self-assembly behavior of amphiphilic block copolymers in the presence of selective solvents to the self-assembly of surfactants in water/oil and the self-assembly of solvent-free block copolymers, and (iii) the repercussions of a and b on aspects both fundamental (e.g., intermolecular and interassembly interactions, thermodynamics of self-assembly) and applied/practical (e.g., formulations for drugs, design of novel materials).

The $(EO)_{19}(PO)_{43}(EO)_{19}-^2H_2O-p$-xylene system exhibits nine different phases, all thermodynamically stable at the same temperature (25 °C): normal micellar cubic, normal hexagonal, normal bicontinuous cubic, lamellar, reverse bicontinuous cubic, reverse hexagonal, and reverse micellar cubic lyotropic liquid crystalline phases, as well as water-rich and water-lean micellar solutions (the total number of phases will be 10 if we add the solvent free $(EO)_{19}(PO)_{43}(EO)_{19}$ copolymer which is in a lamellar state). This is the richest structural polymorphism ever observed in ternary amphiphile-containing mixtures. At the same time, the present is the first report of reverse (water-in-oil) micellar cubic (I_2) and normal (oil-in-water) bicontinuous cubic (V_1) structures in PEO/PEO copolymer systems. The progression (and relative location) of the various phases in the ternary PEO/PPO−water−oil phase diagram is consistent with a decreasing interfacial mean curvature (from the low-left to the low-right corner of Figure 1). This modulation of the interfacial curvature (and the resulting microstructure) can be attributed to the ability of the macromolecular blocks to swell with solvent to a varying extent depending on the amount of solvent(s) available. Both "normal" and "reverse" structures can thus be formed by an amphiphile having a fixed hydrophobe/hydrophile (PPO/PEO) ratio. In addition to the water/oil ratio, the total copolymer content is also important in order for certain phases to form.

The self-assembly of amphiphilic block copolymers in the presence of selective solvent is similar in some aspects to the self-assembly of surfactants in solution (e.g., interfacial curvature modulated by solvent) and in other aspects to the self-assembly of bulk block copolymers in the absence of solvents (e.g., interfacial curvature modulated by block composition). Nevertheless, it, exhibits a number of features (e.g., ability to form both normal and reverse structures at the same temperature with the same block composition) which distinguish it from either the surfactant or the solvent-free block copolymer self-assembly. We can thus consider the ternary phase behavior of the kind described in this paper a new paradigm in self-assembly, as well as a link between the self-assembly of surfactants in water (and oil/cosurfactant) and the self-assembly of dry block copolymers.

(52) Hamley, I. W.; Koppi, K. A.; Rosedale, J. H.; Bates, F. S.; Almdal, K., Mortensen, K. *Macromolecules* **1993**, *26*, 5959.

(53) Hajduk, D. A.; Takenouchi, H.; Hillmyer, M. A.; Bates, F. S.; Vigild, M. E.; Almdal, K. *Macromolecules* **1997**, *30*, 3788.

(54) Hajduk, D. A.; Harper, P. E.; Gruner, S. M.; Honeker, C. C.; Thomas, E. L.; Fetters, L. J. *Macromolecules* **1995**, *28*, 2570.

(55) Qi, S.; Wang, Z.-G. *Macromolecules* **1997**, *30*, 4491.

(56) Laradji, M.; Shi, A.-C.; Noolandi, J.; Desai, R. C. *Macromolecules* **1997**, *30*, 3242.